An EXAFS Investigation of the Coordination Structure of Copper(II) Ions in Aqueous $Cu(ClO_4)_2$ and Methanolic $CuCl_2$ Solutions

Yoshichika TAJIRI and Hisanobu WAKITA*
Department of Chemistry, Faculty of Science, Fukuoka University,
8-19-1, Nanakuma, Jonan-ku, Fukuoka 814-01
(Received February 5, 1986)

The coordination structure of copper(II) ions in aqueous and methanolic solutions was investigated by means of EXAFS spectroscopy. The hexaaquacopper(II) complex in the aqueous $Cu(ClO_4)_2$ solution had an elongated octahedral structure, with four equatorial distances of 2.00 Å and two axial distances of 2.28 Å. Scarcely no axial interaction has been seen in the radial-distribution curve after the Fourier transform of the EXAFS spectrum, for the real and imaginary parts of the Fourier transformed function for the axial interactions are diminished by the interference of those for the equatorial interactions. Two distances for the equatorial interactions of the mixed-ligand chlorocopper(II) complexes in the methanolic $CuCl_2$ solution were clearly resolvable in the radial-distribution curve; they were 2.00 Å and 2.22 Å for the Cu–O and Cu–Cl interactions respectively.

Both EXAFS and X-ray diffraction methods have been used in the structural studies of metal complexes in solution.[1-10] A number of X-ray-diffraction studies have established the elongated octahedral structure of six-coordinated copper(II) complexes in solution.[1-3,7-9] However, only a few EXAFS studies[4,5] have been performed to determine the axial interaction of the octahedral structure in solution.

X-Ray-diffraction investigations have shown that the hexaaquacopper(II) complex in 1.94—3.55 mol dm^{-3} aqueous $Cu(ClO_4)_2$[1,2] and 1.386 mol dm^{-3} aqueous $CuSO_4$[3] solutions has an elongated octahedral structure with four equatorial bonds of 1.94—1.98 Å and two axial bonds of 2.34—2.43 Å, because there exist peaks caused by the $Cu-O_{eq}$ (equatorial) and $Cu-O_{ax}$ (axial) bonds in the radial-distribution function, $D(r)$.

According to Sham et al.,[4] who analyzed the EXAFS spectrum of the K-edge of copper in a 1 mol dm^{-3} aqueous $Cu(ClO_4)_2$ solution, the extremely large values of the axial distance (2.60 Å) and the Debye–Waller factor (0.12 Å) suggested that the axial ligands were loosly bonded. Sano et al.[5] mentioned, in their EXAFS study of a 0.32 mol dm^{-3} aqueous $Cu(ClO_4)_2$ solution, but without detailed analysis, that the second peak appearing at 2.46 Å in the radial-distribution curve corresponds to the $Cu-O_{ax}$ interaction.

X-Ray-diffraction studies of a 2.952 mol dm^{-3} aqueous $CuCl_2$ solution[7] and a 1.016—4.364 mol dm^{-3} aqueous $CuBr_2$ solution[8] disclosed that mixed-ligand six-coordinated aquahalogenocopper(II) complexes had elongated octahedral structures with four bonds including both $Cu-X_{eq}$ (X=Cl,Br) and $Cu-O_{eq}$ and two $Cu-O_{ax}$ bonds, although the peak due to the $Cu-O_{ax}$ bonds did not appear as a separate one. Moreover, 1.055—2.350 mol dm^{-3} methanolic $CuCl_2$ solutions[9] included nearly equivalent amounts of three copper(II) complexes, $[CuCl_n(CH_3OH)_{6-n}]$, where n=1, 2, and 3, although the peaks caused by the $Cu-O_{eq}$, $Cu-Cl_{eq}$, and $Cu-O_{ax}$ bonds overlapped with each other.

Thus far no elongated octahedral structure of aquahalogenocopper(II) complexes in solution has been reported on the basis of EXAFS spectroscopy.[10]

From the consideration of the investigations described above, it seemed that it would be of interest to examine whether or not the EXAFS spectroscopy is able to "see" the axial interaction of the six-coordinated octahedral copper(II) complexes in solution. In the present paper, we attempt to analyze the structures of the copper(II) complexes in 1.019 mol dm^{-3} aqueous $Cu(ClO_4)_2$ and 0.996 mol dm^{-3} methanolic $CuCl_2$ solutions for the purpose of seeing the axial interaction by means of EXAFS spectroscopy. In order to obtain detailed information on the structure, the EXAFS data were analyzed by using not only a conventional curve-fitting method, but also the radial-distribution method to be described in the following Experimental section. The radial-distribution method used in an EXAFS study of a rhodium catalyst by Koningsberger et al.[11] seemed suitable for the analysis of the present EXAFS data, where the interatomic distances are close to each other.

Experimental

EXAFS Measurements. The EXAFS measurements were carried out by the use of synchrotron radiation using the EXAFS facilities at BL-10B of the Photon Factory in the National Laboratory for High-Energy Physics (KEK-PF). The data were collected in the range from ca. 400 eV on the lower-energy side of the Cu absorption K-edge of 8981.83 eV (λ=1.3804 Å) to ca. 1600 eV on the higher-energy side; the time for the data collection was fixed at 1 s at each measuring point.

The reference compounds, bis(acetylacetonato)copper(II) and tetramethylammonium tetrachlorocuprate(II), were prepared by the conventional methods, powdered with an agate mortar, and pressed with polyethylene powder into

films.

An 1.019 mol dm^{-3} aqueous copper(II) perchlorate solution was prepared by dissolving the copper(II) perchlorate in distilled water, which had been obtained by the reaction of copper(II) oxide with a hot perchloric acid solution and recrystallized three times from distilled water. A 0.996 mol dm^{-3} methanolic copper(II) chloride solution was prepared by dissolving copper(II) chloride crystals in absolute methanol. The concentrations of the copper(II) ion in the sample solutions were determined by the EDTA titration method. Each solution sample was put into a polyethylene pouch sandwiched by a polyacrylate holder.

Data Reduction Procedure. The EXAFS spectrum which is extracted from the observed absorption spectrum is expressed by:

$$\chi_{obsd}(k) = [\mu_{obsd}(k) - \mu_0(k)]/\mu_0(k), \quad (1)$$

where $\mu_{obsd}(k)$ is the absorption coefficient, attributed only to the K-edge of the absorption atom and where $\mu_0(k)$ is the smoothly varying background absorption coefficient, approximated by a cubic spline function.[12] k is the photoelectron wave-number and is given as $\sqrt{2m(E-E_0-\Delta E)/h^2}$, where E denotes the energy of the incident X-ray; E_0 is the theoretical energy at the absorption edge for the absorption atom, and ΔE is the correction value for the E_0 value at the absorption edge.

Analysis by the Curve-Fitting Method. The EXAFS spectrum, weighted by k^3, is converted by the Fourier transform into the Fourier transformed function, $F(r)$, in the r-space as:

$$F(r) = \int_{k_{min}}^{k_{max}} k^3 \cdot \chi_{obsd}(k) \cdot \exp(2ikr)dk = ReF(r) + iImF(r). \quad (2)$$

Moreover, the radial distribution function, $|F(r)|$, is given as:

$$|F(r)| = [ReF(r)^2 + ImF(r)^2]^{1/2}, \quad (3)$$

where $ReF(r)$ and $ImF(r)$ are the real and imaginary parts of the $F(r)$ function respectively. The structure parameters (interatomic distances, mean-square displacements, and coordination numbers) are obtained by comparing the Fourier filtered EXAFS spectrum, $\overline{\chi}(k)$, with the calculated EXAFS spectrum, $\chi_{calcd}(k)$. $\overline{\chi}(k)$ is obtained by performing the Fourier backfiltering of the peak in the $|F(r)|$ curve into the EXAFS spectrum in the k-space, while $\chi_{calcd}(k)$ is given by the single-scattering theory[13] as:

$$\chi_{calcd}(k) = \sum_j [N_j/(k \cdot R_j^2)] \cdot |f_j(\pi, k)| \cdot \sin(2kR_j + \phi_j(k)) \cdot \exp(-2R_j/\gamma) \cdot \exp(-2\sigma_j^2 k^2), \quad (4)$$

where R_j and N_j are the distance from the absorbing atom to the j-th coordination shell and the number of atoms at R_j respectively, where σ_j^2 is the mean square displacement[14] of R_j, and γ is the mean free path. $|f_j(\pi,k)|$ and $\phi_j(k)$ are the backscattering amplitude and the phase shift of the atoms in the j-th backscattering shell respectively. A curve fitting is applied to minimize the error-square sum, U ($=\sum[k^3 \cdot \overline{\chi}(k) - k^3 \cdot \chi_{calcd}(k)]^2$).

Analysis by the Radial-Distribution Method. The analysis of this method[11] is performed by using the Fourier transformed function, $F'(r)$, which is corrected for the phase shift and the backscattering amplitude as:

$$F'(r) = \int_{k_{min}}^{k_{max}} [k \cdot \chi(k)/|f(\pi, k)|] \cdot \exp(2ikr + \phi(k))dk = ReF'(r) + iImF'(r), \quad (5)$$

and using the radial-distribution function, $|F'(r)|$, given as:

$$|F'(r)| = [ReF'(r)^2 + ImF'(r)^2]^{1/2}. \quad (6)$$

The optimal values of the structure parameters are obtained by comparing the peak in the calculated $|F'(r)|$ curve with that in the observed $|F'(r)|$ curve in order to minimize the disagreement of the peak-height, -width, and -position. The calculated $|F'(r)|$ curve is obtained from $\chi_{calcd}(k)$ by the Fourier transform according to Eqs. 5 and 6, where $\chi_{calcd}(k)$ is given by substituting j (=1), γ (the initial value in the present paper, 5.0), and the initial values of the structure parameters (taken from the literature) in Eq. 4. The γ, N, R, and σ^2 parameters are allowed to vary at intervals of 0.02, 0.01, 0.001 Å, and 0.0001 $Å^2$ respectively.

If the EXAFS spectrum comes from one interaction, the peak in the $|F'(r)|$ curve as corrected for the phase shift and backscattering amplitude of the interaction, should coincide in position with the maximum peak in the $ImF'(r)$ oscillation.[12,15] In addition, the main peak in the $|F'(r)|$ curve and the $ImF'(r)$ oscillation should be almost symmetrical with respect to the ordinate at the position of the coincidence.[15] On the other hand, if the $|F'(r)|$ curve is inappropriately corrected for the phase shift and backscattering amplitude by taking an improper interaction into consideration, the maximum peak in the $ImF'(r)$ oscillation can not coincide in position with that in the $|F'(r)|$ curve. If the EXAFS spectrum arises from two interactions or more, the $ImF'(r)$ oscillation can be asymmetrical with respect to the ordinate around the maximum peak. The analysis of the peaks in the $|F'(r)|$ curve is as follows. The first step is to estimate the values of the structure parameters of one interaction which peaks more clearly than the other interactions in the $|F'(r)|$ curve. The next step is to subtract the $\chi_{calcd}(k)$ spectrum from the $\chi_{obsd}(k)$ spectrum. This subtraction gives the residual EXAFS spectrum, $\chi_{res}(k)$, in which the contribution of other interactions is included. Then, the third step is to analyze the peak in the $|F'(r)|$ curve of the $\chi_{res}(k)$ in a way similar to that described above by but using another set of structural parameters for an additional interaction in order to obtain the best-fit function of $\chi'_{calcd}(k)$. If a difference between the peak in the $|F'(r)|$ of the $\chi_{res}(k)$ and that of the $\chi'_{calcd}(k)$ still remains, the analysis should be repeated in a similar way by assuming further interactions.

The curve-fitting method is carried out by comparing the $\overline{\chi}(k)$ with the $\chi_{calcd}(k)$ spectra in the k-space; it needs an additional Fourier backfiltering of the peak in the $|F(r)|$ curve. On the other hand, the radial-distribution method compares the observed $|F'(r)|$ value with the calculated $|F'(r)|$ curves in the r-space and necessitates a Fourier transform of the $\chi_{calcd}(k)$. Theoretically, therefore, the two methods should give equivalent results.

Results and Discussion

Reference Compounds. The analysis of the EXAFS data makes it necessary to estimate the phase shift and the backscattering amplitude. In the present study, the phase shift and the backscattering amplitude are determined experimentally by the use of approximated equations.[16,17] The EXAFS spectra of two reference compounds, powdered $Cu(acac)_2$ (acac = acetylacetonate ion) and $[(CH_3)_4N]_2[CuCl_4]$ crystals, with known structures[18,19] were measured in order to estimate the phase shifts and backscattering amplitudes of the copper-oxygen and copper-chlorine interactions. The EXAFS spectrum, $k^3 \cdot \chi_{obsd}(k)$, and the radial distribution curve, $|F(r)|$, for the $Cu(acac)_2$ crystal are shown in Figs. 1-A and 1-B, and those for the $[(CH_3)_4N]_2[CuCl_4]$ crystal, in Figs. 1-C and 1-D. Judging from the crystal structures of these two reference compounds, we considered that the first peak in Figs. 1-B and 1-D corresponds to the first backscattering shell around the Cu^{2+} ion. Therefore, the first peak at 1.56 Å in Fig. 1-B is attributed to the interaction between copper and oxygen atoms within coordinated acetylacetonate ions,[18] while the first peak at 1.86 Å in Fig. 1-D is ascribed to the interaction between copper and chlorine atoms.[19] Performing the Fourier backfiltering over the region of the first peak in each $|F(r)|$ curve, we carried out the curve-fitting in order to obtain the phase shifts and backscattering amplitudes, using known coordination numbers and bond distances. The ΔE and γ values were fixed at 0.0 eV and 5.0 respectively, while σ^2 was allowed to vary. The crystallographic data and Fourier transform range of the reference compounds are summarized in Table 1.

Aqueous $Cu(ClO_4)_2$ Solution. The $k^3 \cdot \chi_{obsd}(k)$ spectrum and the $|F(r)|$ curve for the aqueous $Cu(ClO_4)_2$ solution are depicted in Figs. 2-A and 2-B respectively. The clear peak at 1.6 Å in the $|F(r)|$ curve can be attributed to the interaction between copper and water oxygen atoms at the equatorial site, for the first shell around the Cu^{2+} ion in this solution corresponds to the $Cu-O_{eq}$ interaction, judging from the results of X-ray diffraction.[1,2] The difference in value between the peak position in the $|F(r)|$ curve and the bond distance of the $Cu-O_{eq}$ obtained by X-ray diffraction[1] (1.94 Å) is −0.34 Å. If we use this value as the correction value for the peak position in the $|F(r)|$ curve, a peak due to the interaction between copper and water oxygen atoms at the axial site (2.43 Å, from X-ray diffraction[1]) should appear at 2.09 Å in the $|F(r)|$ curve. However, the peak found at ca. 2.1 Å is too small to be attributed to the $Cu-O_{ax}$ interaction. If the peak due to the $Cu-O_{ax}$ interaction

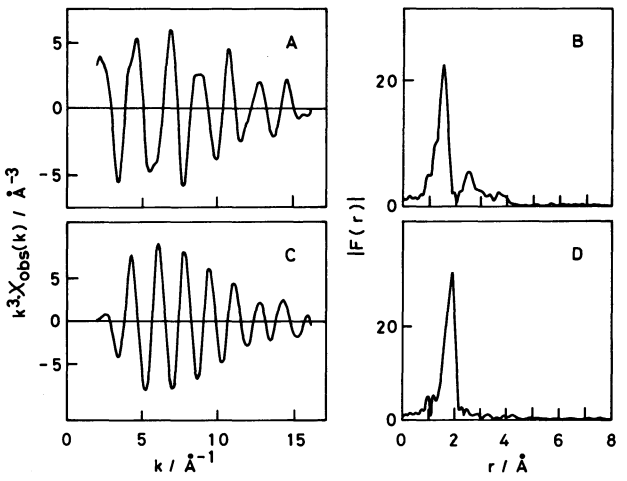

Fig. 1. The EXAFS spectra, $k^3 \cdot \chi_{obsd}(k)$ and the radial distribution curves, $|F(r)|$ for the reference compounds. A, C: $k^3 \cdot \chi_{obsd}(k)$. B, D: $|F(r)|$. A, B: $[Cu(acac)_2]$ crystal. C, D: $[(CH_3)_4N]_2[CuCl_4]$ crystal.

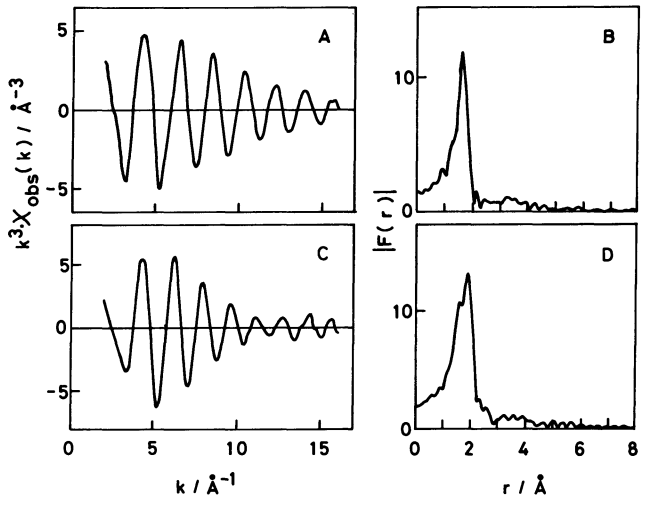

Fig. 2. The EXAFS spectra, $k^3 \cdot \chi_{obsd}(k)$ and the radial distribution curves, $|F(r)|$ for the solution samples. A, C: $k^3 \cdot \chi_{obsd}(k)$. B, D: $|F(r)|$. A, B: aqueous $Cu(ClO_4)_2$ solution. C, D: methanolic $CuCl_2$ solution.

Table 1. Crystallographic Data and Ranges of Fourier Transforms of the Reference Compounds

Sample	k_1-range	r-range	k_2-range	N_{ref}	R_{ref}
$Cu(acac)_2$	3.0—17.0	0.80—1.90	4.5—16.0	4.0	1.95
$[(CH_3)_4N]_2[CuCl_4]$	3.0—18.0	1.11—2.22	4.5—15.0	4.0	2.22

k_1-range: the range of the Fourier transform, $Å^{-1}$; r-range: the range of the Fourier backfiltering, Å; k_2-range: the range of the curve-fitting, $Å^{-1}$; N_{ref}: coordination number; R_{ref}: interatomic distance, Å.

is small and widespread in the r-space, the peaks caused by the Cu–O_{eq} and Cu–O_{ax} interactions might not be clearly resolvable in the $|F(r)|$ curve because the bond distances of the two interactions are too close to each other. On the basis of this consideration, the curve-fitting analysis of the EXAFS data of this solution was carried out in the following way.

Performing the Fourier backfiltering over the region around the first peak (from 0.93 Å to 2.69 Å) in the $|F(r)|$ curve, we carried out the curve-fitting analysis by assuming two models; one corresponds to a two-shell model which has a six-coordinated elongated octahedral structure, as has been proposed on the basis of the results of X-ray diffraction,[1,2] while the other corresponds to a one-shell model which has a square-planar structure with four Cu–O_{eq} interatomic distances. In the course of the curve-fitting analysis, the coordination numbers were fixed at 4 for the one-shell model and at 6 (N_{eq}=4, N_{ax}=2) for the two-shell model; ΔE was also fixed at 0.0 eV. On the other hand, the γ value was allowed to vary. The γ value thus obtained changed from 5.0 (which was initially determined by the use of the $Cu(acac)_2$ crystal) to 5.4. The results of the curve-fitting analysis are listed in Table 2. The value of the error-square sum obtained from the two-shell model (7.74) is smaller than that from the one-shell model (24.08). As seen in Table 2, the interatomic distances for the Cu–O_{eq} and Cu–O_{ax} interactions obtained from the two-shell model are 2.00 Å and 2.28 Å respectively; these values are slightly different from those of the results reported by Ohtaki et al.,[1] but almost identical with those reported by Magini.[2] The difference in interatomic distance between the X-ray diffraction studies and our EXAFS data analysis may result from the uncertainties in the backscattering amplitude and phase shift used and those in the EXAFS data. The σ^2 values of the Cu–O_{eq} and Cu–O_{ax} interactions obtained are 0.0036 $Å^2$ and 0.0105 $Å^2$ respectively; they are in good agreement with the results obtained by the X-ray diffraction method.[1,14] According to the results reported by Sham et al.,[4] the interatomic distance of the Cu–O_{ax} interaction and the $[\sigma_{ax}^2/\sigma_{eq}^2]$ ratio are 2.60 Å and ca. 10 respectively. These values may be too large compared to the maxima values of the X-ray-diffraction studies (2.5 Å for the interatomic distance of the Cu–O_{ax} interaction[20] and ca. 6.5 for the $[b_{ax}/b_{eq}]$ ratio).[2,14] If the structure parameters obtained by the EXAFS method have the same quality as those obtained by the X-ray-diffraction method, the values obtained by the two methods should be close to each other.

By the theoretical calculation of the $|F(r)|$ curve for the Cu–O_{ax} interaction, which was performed independently of that for the Cu–O_{eq} interaction, the Cu–O_{ax} interaction gave a clear peak in the $|F(r)|$ curve different from that in the observed $|F(r)|$ curve. In the next step, therefore, we performed the radial-distribution analysis of the peaks in the radial-distribution curve in order to examine why the peak due to the Cu–O_{ax} interaction is scarcely seen in the curve and to reconfirm the presence of the peak. Instead of the $|F(r)|$ curve, the $|F'(r)|$ curve was used for the radial-distribution method, which was corrected for the phase shift and the backscattering amplitude. In the course of the radial-distribution analysis, the N_{eq} of the Cu–O_{eq} interaction was fixed at 4, while the γ, R_{eq}, and σ_{eq}^2 values of the Cu–O_{eq} interaction were allowed to vary simultaneously. The optimal γ value thus obtained was 5.4, in good agreement with that obtained by the curve-fitting method. The initial values of the Cu–O_{eq} interaction were 1.94 Å for R_{eq} and 0.004 $Å^2$ for σ_{eq}^2.

In Figs. 3-A and 3-B, the solid lines show the $|F'(r)|$ curve and the $ImF'(r)$ oscillation respectively. The peak caused by the Cu–O_{ax} interaction is scarcely seen at all in Fig. 3-A. In Fig. 3-B, the $ImF'(r)$ oscillation is slightly asymmetrical along the axis passing through the maximum peak at ca. 2.0 Å; that is, the

Table 2. Structure Parameters Obtained by the Analysis of the EXAFS Data of Solution Samples

Sample	Structure model	U	Interaction	Curve-Fitting			Radial-Distribution		
				N	R	σ^2	N	R	σ^2
1.019 mol dm^{-3} aqueous $Cu(ClO_4)_2$ solution	one-shell	24.08	Cu–O_{eq}	4.0[a]	2.00±0.001	0.0037±0.0002			
	two-shell	7.74	Cu–O_{eq}	4.0[a]	2.00±0.001	0.0036±0.0002	4.0[a]	2.00	0.0037
			Cu–O_{ax}	2.0[a]	2.28±0.005	0.0105±0.0007	1.8	2.28	0.0090
0.996 mol dm^{-3} methanolic $CuCl_2$ solution	two-shell	5.93	Cu–O_{eq}	2.0[a]	2.01±0.001	0.0047±0.0003			
			Cu–Cl_{eq}	2.0[a]	2.22±0.001	0.0059±0.0002			
	three-shell	5.92	Cu–O_{eq}	2.0[a]	2.01±0.001	0.0047±0.0003	2.0[a]	2.00	0.0047
			Cu–Cl_{eq}	2.0[a]	2.22±0.001	0.0059±0.0002	2.0[a]	2.22	0.0059
			Cu–O_{ax}	2.0[a]	2.28±0.711	0.0872±0.2672			

a) Fixed, N: coordination number, R: interatomic distance; Å, σ^2: mean square displacement of R; $Å^2$, U: error square sum ($=\sum[k^3\cdot\bar{\chi}(k)-k^3\cdot\chi_{calcd}(k)]^2$); $Å^{-6}$.

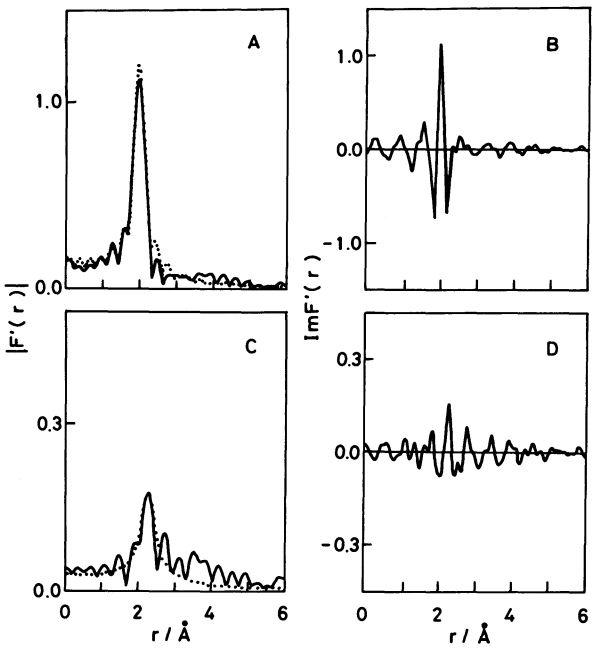

Fig. 3. The corrected radial distribution curves, $|F'(r)|$ and the imaginary parts, $ImF'(r)$ for the aqueous $Cu(ClO_4)_2$ solution. A: $|F'(r)|$ of the $\chi_{obsd}(k)$ (solid line), the $\chi_{calcd}(k)$ of the Cu–O_{eq} interaction (dotted line). B: $ImF'(r)$ of the $\chi_{obsd}(k)$. C: $|F'(r)|$ of the $\chi_{res}(k)$ (solid line), the $\chi_{calcd}(k)$ of the Cu–O_{ax} interaction (dotted line). D: $ImF'(r)$ of the $\chi_{res}(k)$.

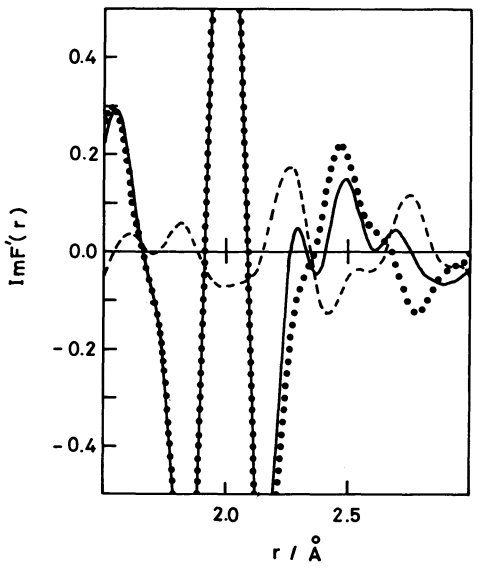

Fig. 4. The imaginary part, $ImF'(r)$ of the corrected Fourier transformed function for the aqueous $Cu(ClO_4)_2$ solution. The $ImF'(r)$ of the $\chi_{obsd}(k)$ (solid line), the $\chi_{calcd}(k)$ of the Cu–O_{eq} interaction (dotted line), and the $\chi_{res}(k)$ (dashed line).

height of the peak at ca. 2.3 Å is lower than that of the peak at ca. 1.6 Å. In Fig. 3-A, the dotted line depicts the $|F'(r)|$ curve of the $\chi_{calcd}(k)$ calculated from the optimal values of the structure parameters of the Cu–O_{eq} interaction. These optimal values were obtained in the r-range below about 2.0 Å in the way described in the Experimental section. When the $|F'(r)|$ curve of the $\chi_{obsd}(k)$ is compared with that of the $\chi_{calcd}(k)$, a small but clear difference is seen at ca. 2.3 Å. To analyze this difference, the residual EXAFS spectrum, $\chi_{res}(k)$, was obtained by subtracting the $\chi_{calcd}(k)$ due to the Cu–O_{eq} interaction from the $\chi_{obsd}(k)$. In Figs. 3-C and 3-D, the solid lines show the $|F'(r)|$ curve and the $ImF'(r)$ oscillation of the $\chi_{res}(k)$ respectively. As the maximum peak of the $ImF'(r)$ oscillation in Fig. 3-D coincided in position with the peak in the $|F'(r)|$ curve in Fig. 3-C, the peak at ca. 2.3 Å can be ascribed to the copper-oxygen interaction. Moreover, from the analysis of this peak, we concluded that this peak was caused by the Cu–O_{ax} interaction, for the coordination number obtained was about 2. Here, the initial values for N_{ax}, R_{ax}, and σ_{ax}^2 were 2, 2.43 Å, and 0.01 Å^2 respectively; they were allowed to vary simultaneously, while γ was fixed at 5.4. In Fig. 3-C, the dotted line shows the $|F'(r)|$ curve of the $\chi_{calcd}(k)$ of the Cu–O_{ax} interaction. The parameter values of this interaction were obtained in the r-range below about 3.0 Å. The results of the radial-distribution method are listed in Table 2. The structure parameters obtained by this method are in good agreement with those obtained by means of the curve-fitting method.

The results of the radial-distribution method were as follows: in the case of the EXAFS spectrum corresponding to two interactions or more, the observed $ImF'(r)$ (or $ReF'(r)$) is the sum of all the $ImF'(r)$ (or $ReF'(r)$) values. If an EXAFS spectrum comes from two interactions, and if the $ImF'(r)$ oscillation due to one interaction has a sign opposite from that of the other interaction at the position of the maximum peak in the latter $ImF'(r)$ oscillation, the latter $ImF'(r)$ oscillation is reduced by the former one. Figure 4 shows the $ImF'(r)$ oscillations of the $\chi_{obsd}(k)$ (solid line), the $\chi_{calcd}(k)$ of the Cu–O_{eq} interaction (dotted line),[15] and the $\chi_{res}(k)$ (dashed line). At ca. 2.3 Å, the dashed line depicts a larger positive peak than that of the solid line, for the dashed line was obtained by subtracting the dotted line (largely negative) from the solid line (barely positive). From a comparison of the $ImF'(r)$ oscillations, we can conclude that the $ImF'(r)$ oscillation due to the Cu–O_{ax} interaction is diminished at the position of the peak due to the Cu–O_{ax} interaction in the radial-distribution curve by the interference of the $ImF'(r)$ oscillation due to the Cu–O_{eq} interaction; consequently, the peak caused by the Cu–O_{ax} interaction can scarcely be seen in the radial-distribution curve.

Methanolic $CuCl_2$ Solution. The $k^3 \cdot \chi_{obsd}(k)$ value and the $|F(r)|$ curve for the 0.996 mol dm^{-3} methanolic $CuCl_2$ solution are shown in Figs. 2-C and 2-D

respectively. According to the results of an X-ray-diffraction study of the methanolic $CuCl_2$ solution,[9] the interatomic distances of the Cu–O_{eq}, Cu–Cl_{eq}, and Cu–O_{ax} interactions are very similar; hence, the corresponding peaks overlap with one another in the radial-distribution function, $D(r)$. However, the $|F(r)|$ curve for the methanolic $CuCl_2$ solution seems to show a double peak in Fig. 2-D. When two back-scattering shells consist of the same number of atoms, but of different kinds, these two distinct absorber-scatterer distances should be resolvable in the $|F(r)|$ curve as separate peaks. Therefore, the peak at ca. 1.9 Å can be attributed to the Cu–Cl interaction, because the position of this peak is close to that in the reference $[(CH_3)_4N]_2[CuCl_4]$ crystal (1.86 Å). Moreover, the shoulder at ca. 1.6 Å of this double peak may be ascribed to the interaction between copper and methanol oxygen atoms at the equatorial site, because the position of this shoulder is close to that in the reference $Cu(acac)_2$ crystal. Similarly to the aqueous $Cu(ClO_4)_2$ solution, the peak due to the Cu–O_{ax} interaction in this solution could scarcely be seen in the $|F(r)|$ curve as a separate peak. Therefore, performing the Fourier backfiltering over the region around this double peak (from 0.95 Å to 3.00 Å), we carried out the curve-fitting analysis by assuming two models; one was a three-shell model which had the same six-coordinated elongated octahedral structure as the results of the X-ray diffraction investigation,[9] while the other was a two-shell model which had a four-coordinated structure with two Cu–O and two Cu–Cl interatomic distances. In the course of the curve fitting, the coordination numbers for those interactions were fixed at 2. The results of the curve-fitting analysis are listed in Table 2. As may be seen in Table 2, the curve-fitting analysis of these two models gave similar error-square sums. Therefore, at this step, we could not conclude whether or not the average structure of the mixed-ligand copper(II) complexes in this solution was an elongated octahedron. The radial-distribution method was, therefore, used for the analysis of this solution.

In the course of the radial-distribution analysis, the coordination numbers for both Cu–O_{eq} and Cu–Cl_{eq} interactions were fixed at 2, while the γ, R, and σ^2 values for each interaction were allowed to vary. The initial values of the Cu–Cl_{eq} interaction were 2.22 Å for R and 0.006 Å^2 for σ^2. In Figs. 5-A and 5-B, the solid lines show the $|F'(r)|$ curve and the $ImF'(r)$ oscillation of the $\chi_{obsd}(k)$ value respectively. The γ value changed from 5.0 (initially determined by the $[(CH_3)_4N]_2[CuCl_4]$ crystal) to 5.4. The Cu–O_{eq} bond length may differ by only ca. 0.2 Å from the Cu–Cl_{eq} one, and the Cu–Cl_{eq} and Cu–O_{ax} interatomic distances are very close to each other; therefore, we first estimated the structure parameters for the Cu–Cl_{eq} interaction because the peak due to the

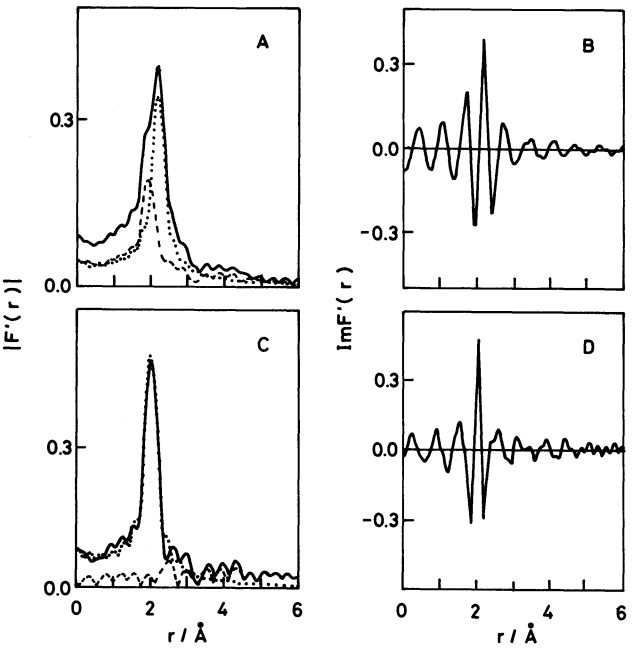

Fig. 5. The corrected radial distribution curves, $|F'(r)|$ and the imaginary parts, $ImF'(r)$ for the methanolic $CuCl_2$ solution. A: $|F'(r)|$ of the $\chi_{obsd}(k)$ (solid line), the $\chi_{calcd}(k)$ of the Cu–Cl_{eq} interaction (dotted line), and the $\chi_{res}(k)$ (dashed line). B: $ImF'(r)$ of the $\chi_{obsd}(k)$. C: $|F'(r)|$ of the $\chi_{res}(k)$ (solid line), the $\chi_{calcd}(k)$ of the Cu–O_{eq} interaction (dotted line), and the $\chi_{rem}(k)$ (dashed line). D: $ImF'(r)$ of the $\chi_{res}(k)$.

Cu–Cl_{eq} interaction was larger and clearer than those due to other interactions. Figure 5-A shows the $|F'(r)|$ curves of the $\chi_{calcd}(k)$ of Cu–Cl_{eq} interaction (dotted line) and the $\chi_{res}(k)$ (dashed line). The structural parameter values of the Cu–Cl_{eq} interaction were obtained in the r-range from ca. 2.0 Å to ca. 3.0 Å. In the $|F'(r)|$ curve of the $\chi_{res}(k)$, there existed a clear peak at ca. 2.0 Å (dashed line). From the value of this peak-position, the main contribution to this peak can be attributed to the Cu–O_{eq} interaction. Therefore, the initial values for the analysis of this peak were 1.95 Å for R and 0.004 Å^2 for σ^2. The γ value was fixed at 5.4, while R and σ^2 were allowed to vary. Figures 5-C and 5-D depict the $|F'(r)|$ curve (solid line) and the $ImF'(r)$ oscillation of the $\chi_{res}(k)$ value respectively. In Fig. 5-C, the dotted line shows the $|F'(r)|$ curve of the $\chi_{calcd}(k)$ of Cu–O_{eq} interaction, while the dashed line shows that of the remaining EXAFS spectrum, $\chi_{rem}(k)$, which is yielded by subtracting the $\chi_{calcd}(k)$ of the Cu–O_{eq} interaction from the $\chi_{res}(k)$ value. The parameter values of the Cu–O_{eq} interaction were obtained in the r-range below about 2.0 Å. A small peak around 2.4 Å in the $|F'(r)|$ curve of the $\chi_{rem}(k)$ was analyzed using the initial values of N(=2), R(=2.4 Å), and σ^2(=0.01 Å^2), where γ was fixed at 5.4, while N, R, and σ^2 were allowed to vary. The coordination number obtained

from this analysis (in the r-range from 2.2 Å to 2.6 Å) was not more than 0.3; therefore, we could not conclude that this small peak is caused by the $Cu-O_{ax}$ interaction. The results of the radial-distribution method are listed in Table 2, without the values of the $Cu-O_{ax}$ interaction.

The results obtained by the use of this method for the equatorial interactions are in good agreement with those obtained by the use of the curve-fitting method, and the values of the structure parameters obtained from both methods support well those of the X-ray diffraction study.[9] However, neither method showed any clear evidence of the $Cu-O_{ax}$ interactions of the mixed-ligand chlorocopper(II) complexes in this solution, in contrast to that of the hexaaquacopper(II) complex in the aqueous $Cu(ClO_4)_2$ solution; therefore, we could not determine whether or not the average structure of the copper(II) complexes in this solution is an elongated octahedron. Presumably, this fact results from the $Cu-Cl_{eq}$ bond length in this solution, which is very close to the $Cu-O_{ax}$ bond length, also, the former bond contributes to a large extent to the EXAFS spectrum, while the $Cu-O_{ax}$ interactions in this solution contribute to the spectrum to only a small extent. Accordingly, it might be difficult to analyze such a small contribution as that of the $Cu-O_{ax}$ interaction in this solution by means of the radial-distribution method, because the estimated errors for the structure parameters, i.e., N, R, and σ^2, of an interaction increase with an increase in the number of peaks caused by other interactions which should be subtracted.

The present EXAFS data analyses by using both methods gave similar results. The radial-distribution method is able to show an anticipated and clear peak in the $|F'(r)|$ curve as evidence of the interaction, which is diminished by the interference of other interactions. Consequently, a combined use of these two methods seems useful for further EXAFS analysis.

Sham et al.[4] explained that the diminishment of the peak due to the $Cu-O_{ax}$ interaction in an aqueous $Cu(ClO_4)_2$ solution results from the interaction having a large σ value. However, a preferable explanation may be that the diminishment of the peak due to the $Cu-O_{ax}$ interaction is caused by the interference between the imaginary and real parts of the Fourier-transformed function of the $Cu-O_{ax}$ interaction and those of the $Cu-O_{eq}$ interaction.

The authors are grateful to Professor Hitoshi Ohtaki and Dr. Toshio Yamaguchi for their valuable discussion and advice. The authors also wish to thank to Dr. Masaharu Nomura for his help and advice in the EXAFS measurements.

References

1) H. Ohtaki and M. Maeda, *Bull. Chem. Soc. Jpn.*, **47**, 2197 (1974).
2) M. Magini, *Inorg. Chem.*, **21**, 1535 (1982).
3) H. Ohtaki, T. Yamaguchi, and M. Maeda, *Bull. Chem. Soc. Jpn.*, **49**, 701 (1976).
4) T. K. Sham, J. B. Hastings, and M. L. Perlman, *Chem. Phys. Lett.*, **83**, 391 (1981).
5) M. Sano, K. Taniguchi, and H. Yamatera, *Chem. Lett.*, **1980**, 1285.
6) M. Sano, T. Maruo, and H. Yamatera, *Bull. Chem. Soc. Jpn.*, **56**, 3287 (1983).
7) M. Magini, *J. Chem, Phys.*, **74**, 2523 (1981).
8) M. Ichihashi, H. Wakita, T. Mibuchi, and I. Masuda, *Bull. Chem. Soc. Jpn.*, **55**, 3160 (1982).
9) M. Ichihashi, H. Wakita, and I. Masuda, *Bull. Chem. Soc. Jpn.*, **56**, 3761 (1983).
10) G. Galli, G. Maisano, P. Migliardo, C. Vasi, F. Wanderlingh, and M. P. Fontana, *Solid State Commun.*, **42**, 213 (1982).
11) This method was not named in their papers, but one of the authors, J. B. A. D. van Zon, called this "modelling" in his Ph. D. Thesis. From the classification of the analytical methods of the EXAFS spectra, we call this method the "radial-distribution method" in this paper; T. Yokoyama, *Kagaku To Kogyo*, **38**, 631 (1985); H. F. J. van't Blik, J. B. A. D. van Zon, T. Huizinga, J. C. Vis, D. C. Koningsberger, and R. Prins, *J. Phys. Chem.*, **87**, 2264 (1983); J. B. A. D. van Zon, D. C. Konigsberger, H. F. J. van't Blik, R. Prins, and D. E. Sayers, *J. Chem. Phys.*, **80**, 3914 (1984); H. F. J. van't Blik, J. B. A. D. van Zon, D. C. Koningsberger, and R. Prins, *J. Mol. Catal.*, **25**, 379 (1984); J. B. A. D. van Zon, Ph. D. Thesis, Eindhoven University of Technology, Eindhoven, The Netherlands (1984).
12) For details of the data treatments, refer to the following literature: I. Masuda, H. Wakita, Y. Tajiri, and M. Ichihashi, *Fukuoka Univ. Sci. Rep.*, **13**, 63 (1983); H. Wakita, Y. Tajiri, and S. Yamashita, *Fukuoka Univ. Sci. Rep.*, **15**, 109 (1985).
13) D. E. Sayers, E. A. Stern, and F. W. Lytle, *Phys. Rev. Lett.*, **27**, 1204 (1971); E. A. Stern, *Phys. Rev.*, **B10**, 3027 (1974).
14) We assumed that the σ value is equivalent to the root mean-square-amplitude, $\langle\Delta r\rangle$, of the X-ray diffraction method, as $\sigma=\langle\Delta r\rangle$ and $b=\sigma^2/2$, where b is the temperature factor of the X-ray diffraction method.
15) Strictly speaking, the symmetry of the main peak in the $|F'(r)|$ curve and that of the $ImF'(r)$ oscillation had been slightly broken by the truncation effect of the Fourier transform; P. A. Lee and G. Beni, *Phys. Rev.*, **B15**, 2862 (1977).
16) B. K. Teo, P. A. Lee, A. L. Simons, P. Eisenberger, and B. M. Kincaid, *J. Am. Chem. Soc.*, **99**, 3854 (1977).
17) P. A. Lee, B. K. Teo, and A. L. Simons, *J. Am. Chem. Soc.*, **99**, 3856 (1977).
18) H. Koyama, Y. Saito, and H. Kuroya, *J. Inst. Polytech. Osaka City Univ.*, **C4**, 43 (1953).
19) B. Morosin and E. C. Lingafelter, *J. Phys. Chem.*, **65**, 50 (1961).
20) H. Ohtaki, "Youeki Kagaku," Shokabo, Tokyo (1985), p. 143.